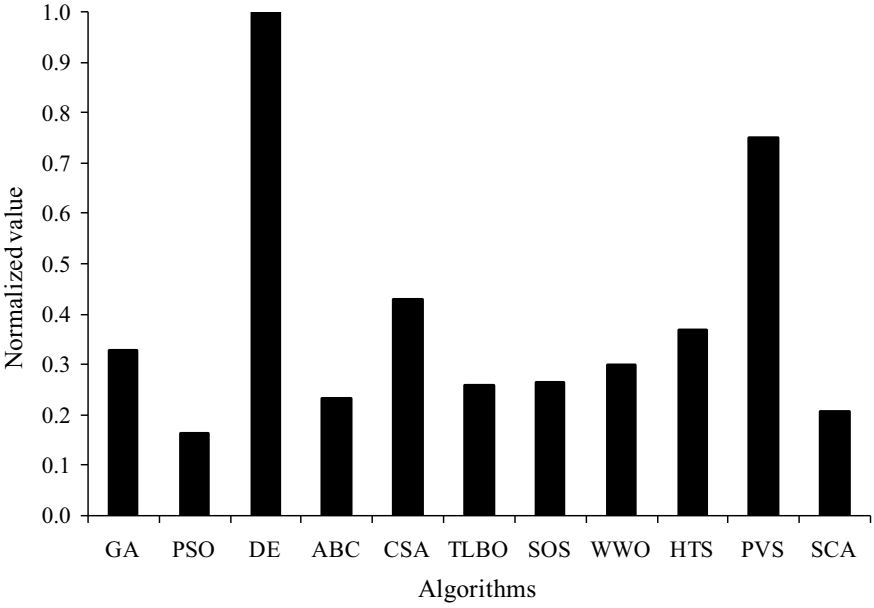

Fig. 3.3 Graphical presentation of Friedman rank test for STHE optimization

3.2 Plate-Fin Heat Exchanger (PFHE)

Plate-fin heat exchanger (PFHE) belongs to the category of compact heat exchanger due to its large heat transfer surface area per unit volume (Kays and London 1984). Plate-fin heat exchangers are widely used in gas–gas applications. As they are used for gas–gas applications, fins provided on both the sides of heat exchangers to increase their surface area in turn increase the heat transfer rate. In PFHEs, plates are separate from each other at some distance in which fins are sandwiched. When hot fluid and cold fluid pass through this heat exchanger, heat transfer takes place through plates and fins.

Plate-fin heat exchangers may be counter-flow type or cross-flow type. Figure 3.4 shows the schematic diagram of cross-flow PFHE. Construction of plate-fin type heat exchanger consists of a number of alternate layers of corrugated metal fins and plates. These are arranged in such a way that it forms a honeycomb structure. Due to this type of structure, it has high resistance to vibration and shock. Bars are provided at edges of plates, which are used to confine each fluid to the space provided between adjacent plates. The whole structure is joined by the brazing process. The different types of fins used in PFHE are plane fin, perforated fin, serrated fin, and herringbone fin.

The plate-fin heat exchanger has large heat transfer surface area per unit volume (because fins are employed on both), high thermal conductivity due to a small thickness of the plate, and high effectiveness (because fins interrupt boundary layer

Table 3.7 The optimized shell and tube heat exchanger design geometry

Operating parameters	Optimized value
Design variables	
Tube outer diameter, d_o (mm)	20.77
Shell diameter, D_s (mm)	446.69
Shell-to-baffle diametrical clearance, d_{sb} (mm)	11.08
Tube-to-baffle diametrical clearance, d_{tb} (mm)	11.19
Tube bundle outer diameter, D_{otl} (m)	0.849
Baffle spacing at center, L_{bc} (mm)	290.33
Baffle spacing at inlet L_{bi} (mm)	108.85
Baffle spacing at the outlet, L_{bo} (mm)	103.59
Baffle cut, B_c (%)	27.96
Tube pitch, P_T (mm)	31.13
Tube layout pattern (°)	60
Number of tubes, N_t	117
Tube length, L(m)	6.6
Number of baffles, N_b	12
Constraints	
Tube-side flow velocity, v (m/s)	1
Tube length/Shell diameter, (L/D_s)	14.78
Surface coefficient, (I_s)	0.25
Pressure drop on the shell side, ΔP_s (Pa)	8.91 × 102
Pressure drop on tube side, ΔP_t (Pa)	5.66 × 103
Objective function	
Operating cost, C_{oc} ($/year)	173.75
Initial cost including interest, C_{cp} ($/year)	5515.1
Total cost, C_{tot} ($/year)	5688.8

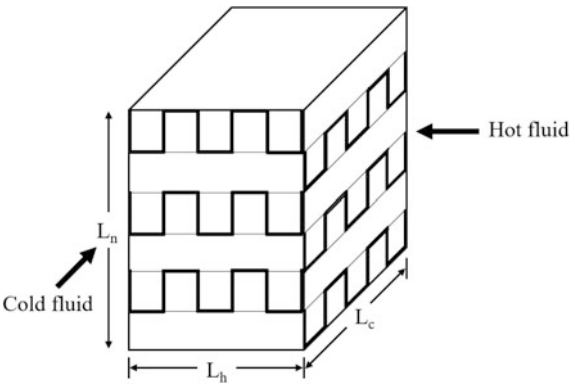

Fig. 3.4 Schematic diagram of cross-flow plate-fin heat exchanger

growth). The above-mentioned characteristics of PFHE result in the reduction of space requirement, weight, and cost (Flamant et al. 2011). However, this greater thermal performance of the PFHE is at the expense of higher pressure drop. Therefore, the optimum design of PFHE always required the trade-off between the thermal and hydraulic performance of the heat exchanger within the given set of constraints. Generally, the objectives involved in the design optimization of PFHE are thermodynamics (i.e., maximum effectiveness, minimum entropy generation rate, minimum pressure drop, etc.), and economics (i.e., minimum cost, minimum weight, etc.).

Earlier, several investigators used various optimization techniques with different methodologies and objective functions to optimize PFHE. In addition to using traditional mathematical methods (Reneaume et al. 2000; Reneaume and Niclout 2003), simulated annealing (Reneaume and Niclout 2001), and artificial neural network (Jia and Sundén 2003), many researchers have successfully employed evolutionary and swarm intelligence-based computation in design optimization of PFHE.

Mishra et al. (2004) and Mishra and Das (2009) used GA for optimal design of plate-fin heat exchangers. The authors considered minimization of the total annual cost and total thermo-economic cost. Peng and Ling (2008) used neural networks cooperated with genetic algorithm for the optimal design of PFHE. The authors considered minimization of weight and minimization of total annual cost as objectives. Xie et al. (2008a, b) applied GA for optimization of plate-fin heat exchangers with minimization of total annual cost as an objective function and pressure drop as a constraint. Peng et al. (2010) used PSO to optimize the structure dimensions of PFHE. The authors considered the total weight and total annual cost minimization of the heat exchanger as an objective function for given constrained conditions. Sanaye and Hajabdollahi (2010a, b) performed a simultaneous optimization of total cost and effectiveness using a design which featured NSGA-II and PFHE. Rao and Patel (2010) carried out thermodynamic optimization of cross-flow plate-fin heat exchanger aiming for minimum entropy generation units of PFHE. Zhang et al. (2010) developed a three-dimensional distributed parameter model for designing the plate-fin heat exchanger. The authors used this model for minimum entropy generation of PFHE. Najafi et al. (2005) carried out multi-objective optimization of PFHE considering the total heat transfer rate and total annual cost of the heat exchanger simultaneously using multi-objective GA. Yousefi et al. (2011) explored the GA hybrid with PSO for optimization of the heat transfer area and pressure drop of the plate-fin heat exchanger. Ghosh et al. (2011) developed a methodology to determine the optimal stacking pattern of multi-stream plate-fin heat exchangers using a genetic algorithm. The authors found out the stacking pattern, which gave the maximum heat load for a given number of fluid streams. Rao and Patel (2011a, b, c) applied teaching–learning-based optimization for the thermodynamic optimization of a plate-fin heat exchanger. Ahmadi et al. (2011) carried out thermo-economic optimization of PFHE using NSGA-II. The authors obtained the Pareto solutions for cost and entropy generation unit of PFHE.

Yousefi et al. (2012a, b) applied the imperialist competitive algorithm (ICA) for optimization of the cross-flow plate-fin heat exchanger. The authors analyzed seven design variables for minimum weight and cost design of PFHE. Yousefi et al. (2012a, b) developed a learning automata-based particle swarm optimization (LAPSO) algorithm for the optimization of PFHE. The efficiency and accuracy of the LAPSO method are demonstrated through the examples of PFHE that included three objectives, namely minimum total annual cost, minimum weight, and a minimum number of entropy generation units. Rao and Patel (2013) performed a multi-objective optimization of PFHE with effectiveness and total cost of the heat exchanger as objective functions. The authors used a modified version of teaching–learning-based optimization (TLBO) algorithm as an optimization tool. Zaho and Li (2013) developed an effective layer pattern optimization model for multi-stream plate-fin heat exchanger using genetic algorithm. Yousefi et al. (2013) proposed a variant of harmony search algorithm for design optimization of plate-fin heat exchangers. The authors demonstrated the efficiency and accuracy of the algorithm by comparing the optimization results with GA and PSO. Zhou et al. (2014) presented an optimization model for PFHE based on entropy generation minimization method. They considered specific entropy generation rate as an objective function and total heat transfer area of PFHE as a constraint. Patel and Savsani (2014) obtained a Pareto front between conflicting thermodynamic and economic objectives of PFHE by implementing multi-objective improved TLBO (MO-ITLBO) algorithm.

Zarea et al. (2014) investigated bees algorithm for the plate-fin heat exchanger optimization. The authors considered maximization of the effectiveness and minimization of entropy generation unit as objective functions in their study. Babaelahi et al. (2014) obtained the Pareto front between thermal and pressure entropy generation units of PFHE with the help of the multi-objective evolutionary algorithm. Hajabdollahi (2015) investigated the effect of nonsimilar fins in the thermo-economic optimization of plate-fin heat exchanger. They considered total annual cost and effectiveness of heat exchanger as objective functions and utilized NSGA-II for optimization. Wang and Li (2015) introduced and applied an improved multi-objective cuckoo search (IMOCS) algorithm for optimization of PFHE. The authors considered conflicting thermo-economic objectives for optimization. Yin and Ooka (2015) performed the structural parameters optimization of a water-to-water plate-fin heat exchanger used in the air-conditioning system. The authors employed GA to obtain single-objective and multi-objective optimization results. Hadidi (2015) employed biogeography-based optimization (BBO) algorithm for optimization of the heat transfer area and total pressure drop of the PFHE. Wang et al. (2015) presented few layer pattern criterion models to determine optimal stacking pattern of the multi-stream plate-fin heat exchanger (MPFHE). The authors developed these models by employing genetic algorithm and observed that the performance of MPFHE in relation to heat transfer and fluid flow was effectively improved by the optimization design of layer pattern. Yousefi et al. (2015)

presented a learning automata-based particle swarm optimization employed to multi-stage thermo-economical optimization of compact heat exchangers.

Wen et al. (2016a, b, c) performed thermodynamic optimization of PFHE. The authors considered two conflicting objectives, namely Colburn factor and friction factor for optimization and used genetic algorithm (GA) as an optimization tool. Du et al. (2016) focused on a double-flow plate-fin heat exchanger for improving its thermal and hydraulic behavior using GA. Turgut (2016) investigated hybrid chaotic quantum behaved particle swarm optimization (HCQPSO) algorithm for minimizing the heat transfer area and total pressure drop of PFHE. Ayala et al. (2016) presented Pareto optimal solution for multi-objective optimization of PFHE by combining free search algorithm with the differential evolutionary algorithm. The authors compared the obtained Pareto front with available Pareto front from NSGA-II. Wen et al. (2016a, b, c) optimized the Colburn factor and friction factor of plate-fin heat exchanges by combining a Kriging response surface and multi-objective genetic algorithm. Segundo et al. (2017) introduced adaptive differential evolution with optional external archive (JADE) and a novel JADE variant, called Tsallis JADE (TJADE) algorithm, for thermodynamic optimization of PFHE. Raja et al. (2017a, b, c) performed the many-objective optimization of the plate-fin heat exchanger by employing heat transfer search algorithm. The authors compared the many-objective optimization results of PFHE with multi-objective optimization results. Cho et al. (2017) optimized layer patterning on a plate-fin heat exchanger for minimum thermal stress using GA. Liu et al. (2017) combined CFD simulation and GA to optimize the design of PFHE. The authors considered the optimization of two conflicting objectives, namely Colburn factor and friction factor of PFHE. Raja et al. (2018a, b) performed thermodynamic as well as thermo-economic optimization of a PFHE by considering the heat transfer search algorithm.

3.2.1 Thermal Model

In the present work, a cross-flow plate-fin heat exchanger with offset strip fin is considered for the optimization. The geometry of PFHE is shown in Fig. 3.4, while the detail of offset strip fin is shown in Fig. 3.5. In this work, the ε-NTU approach is used to predict the performance of PFHE. The PFHE is running under a steady state, and the area distribution and heat transfer coefficients are assumed to be uniform and constant. Further, the thermal–hydraulic model presented here is based on the previous works of Sanaye and Hajabdollahi (2010a, b), Rao and Patel (2013), Patel and Savsani (2014), and Raja et al. (2017a, b, c). Moreover, the subscripts h and c stand for hot side and cold side, respectively, in the different equations of the thermal–hydraulic model.

For the cross-flow heat exchanger with both fluids unmixed, effectiveness (ϵ) is given by Incropera and DeWitt (1998) as follows:

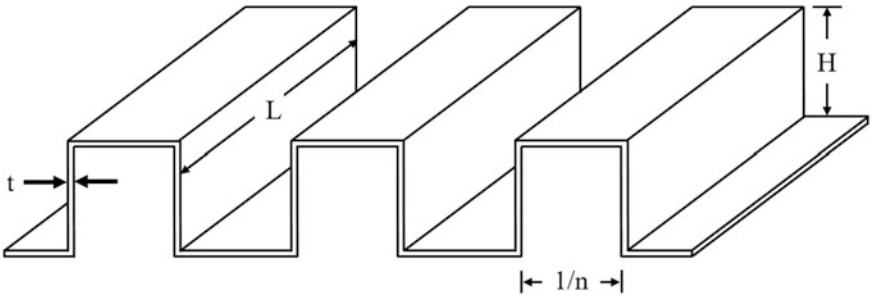

Fig. 3.5 Detailed geometry of offset strip fin

$$\varepsilon = 1 - \exp\left[\left(\frac{1}{C_r}\right)\mathrm{NTU}^{0.23}\left[\exp\left(-C_r\mathrm{NTU}^{0.78}\right) - 1\right]\right] \tag{3.49}$$

where the heat capacity ratio (C_r) is given as

$$C_r = C_{\min}C_{\max} \tag{3.50}$$

where $C_{\min}$ and $C_{\max}$ are the minimum and maximum heat capacity fluids, respectively. The heat of the fluid is given by

$$C = mC_p \tag{3.51}$$

where C_p is the specific heat of the fluid.

The number of transfer units (NTU) is given by the following equation:

$$\frac{1}{\mathrm{NTU}} = \frac{C_{\min}}{\mathrm{UA}} = C_{\min}\left[\frac{1}{(hA)_h} + \frac{1}{(hA)_c}\right] \tag{3.52}$$

where h is the convective heat transfer coefficient, U is the overall heat transfer coefficient, and A is the heat transfer surface area.

Heat transfer areas of the hot and cold sides of the heat exchanger are obtained by

$$A_h = L_hL_cN_h[1 + 2n_h(H_h - T_h)] \tag{3.53}$$

$$A_c = L_hL_cN_h[1 + 2n_c(H_c - T_c)] \tag{3.54}$$

where L_c and L_h indicate cold-side and hot-side flow length, N_h and N_c indicate the number of hot-side and cold-side layer, H_h and H_c indicate fin height on the hot side and cold side, t_h and t_c indicate fin thickness on the hot side and cold side, and n_h and n_c indicate fin frequency on the hot side and cold side, respectively.

Based on the hot side and cold side, the total heat transfer area of the heat exchanger is formulated as

$$A = A_h + A_c = L_h L_c[N_h(1 + 2n_h(H_h - T_h)) + (N_h(1 + 2n_c(H_c - T_c))] \quad (3.55)$$

The free flow area (A_{ff}) for the hot side and cold side of the plate-fin heat exchanger geometry is given by

$$A_{ff,h} = (H_h - t_h)(1 - n_h t_h)L_c N_h \quad (3.56)$$

$$A_{ff,c} = (H_c - t_c)(1 - n_c t_c)L_h N_c \quad (3.57)$$

The heat transfer coefficient of the plate-fin heat exchanger is given by

$$h = jGC_P(pr)^{-0.667} \quad (3.58)$$

where j is the Colburn factor, Pr is the Prandtl number, and G is the mass flux velocity and are obtained using the following equations:

$$Pr = \frac{\mu C_p}{k} \quad (3.59)$$

$$G = \frac{m}{A_{ff}} \quad (3.60)$$

where μ and k are the viscosity and thermal conductivity of the fluids, respectively.

The Colburn factor required to calculate the heat transfer coefficient is obtained by the correlation given by Manglik and Bergles (1995),

$$j = \left(0.6522(Re)^{-0.5403}(\alpha)^{-0.1541}(\delta)^{0.1499}(\gamma)^{-0.0678}\left[1 + 5.269 \times 10^{-5}(Re)^{1.34}(\alpha)^{0.504}(\delta)^{0.456}(\gamma)^{-1.055}\right]\right)^{0.1} \quad (3.61)$$

where Re is the Reynolds number; α, δ, and γ are dimensionless parameters and are given by

$$Re = \frac{Gd_h}{\mu} \quad (3.62)$$

$$\alpha = \frac{f_s}{H - T} \quad (3.63)$$

$$\delta = \frac{t}{l_f} \quad (3.64)$$

$$\gamma = \frac{t}{f_s} \tag{3.65}$$

$$f_s = \left(\frac{1}{n} - t\right) \tag{3.66}$$

where f_s is the fin spacing, l_f is the lance length of the fin, and d_h is the hydraulic diameter and are calculated by the below equation.

$$d_h = \frac{4fsl_f(H-T)}{2\left(fsl_f + (H-T)l_f + (H-T)t\right) + tfs} \tag{3.67}$$

The pressure drop of both the fluid streams of the plate-fin heat exchanger is obtained using the correlation given by Shah and Sekulic (2003a, b) as

$$\Delta P_h = \frac{2f_h L_h G_h^2}{\delta_h d_{h,h}} \tag{3.68}$$

$$\Delta P_c = \frac{2f_c L_c G_c^2}{\rho_c d_{h,c}} \tag{3.69}$$

where f is the friction factor and is obtained by the following equation:

$$f = (9.6243(Re)^{-0.7422}(\alpha)^{-0.1856}(\delta)^{0.3053}(\gamma)^{-0.2659}\left[1 + 7.669 \times 10^{-8}(Re)^{4.429}(\alpha)^{0.920}(\delta)^{3.767}(\gamma)^{0.236}\right)^{0.1} \tag{3.70}$$

The above thermal–hydraulic model of PFHE is used for the cost estimation of the heat exchanger.

(a) **Cost estimation**

The total cost (C_{tot}) of a heat exchanger includes the capital cost (C_{cp}) and the operating cost (C_{oc}) of the device. The capital cost of a heat exchanger is estimated from the following correlation:

$$C_{cp} = A_{cf} C_A A^{n_1} \tag{3.71}$$

where C_A is the cost per unit surface area, n_1 is the exponent of nonlinear increase with area increase, and A_{cf} is the annual coefficient factor and is calculated by

$$A_{cf} = \frac{\text{roi}}{1 - (1 + \text{roi})^{-Z_1}} \tag{3.72}$$

where roi and z_1 represent interest rate and depreciation time, respectively.

The operating cost is governed by pumping power required for driving the hot and cold fluids through the exchanger and is calculated by

$$C_{\mathrm{op}} = \left[\zeta\tau\frac{\Delta PV}{\eta\rho}\right]_{\mathrm{h}} + \left[\zeta\tau\frac{\Delta PV}{\eta\rho}\right]_{\mathrm{c}} \tag{3.73}$$

where V is the volumetric flow rate of the fluid, ζ is the electricity price, τ is the hours of operations, and η is the compressor efficiency.

So, the total annual cost of the PFHE is given by

$$C_{\mathrm{tot}} = C_{\mathrm{cp}} + C_{\mathrm{op}} \tag{3.74}$$

The above-mentioned cost estimation is used to calculate the objective function of the case study described in the next section.

3.2.2 *Case Study, Objective Function Description, and Constraints*

A gas-to-air single-pass cross-flow plate-fin heat exchanger is needed in order to design and optimize the minimum total annual cost. The heat duty of the heat exchanger is 1069.8 kW. The hot flow, cold flow, and no flow length of the heat exchanger are 1, 1, and 1.5 m, respectively. The offset strip fin is employed on both the sides of heat exchanger. Specifications of offset strip fin on both the sides of the heat exchanger are identical. The PFHE is constructed from the aluminum with a density of 2700 kg/m^3. The maximum allowable pressure drop on the hot side is 9.5 kPa and on the cold side is 8 kPa. The mass flow rate and temperature of the fluids are considered as design specifications. Hot-side flow length (L_{h}), cold-side flow length (L_{c}), fin height (H), fin thickness (t), fin frequency (n), lance length of fin (l_{f}), and the number of hot-side layers (N_{h}) are considered as design variables which are needed to optimize the minimum total cost of the heat exchanger. Table 3.8 presents the operating conditions of PFHE, which is supplied as an input to the heat exchanger case study. The lower bound and upper bound of the design variables are listed in Table 3.9, while Figs. 3.4 and 3.5 indicates the heat exchanger geometry along with the design variables. Further, all the parameters required for cost evaluations are presented in Table 3.10.

As mentioned above, minimization of the total cost (C_{tot}) of the PFHE is taken as an objective function in the present study. Further, the heat exchanger geometry which results in minimum total cost also satisfies the pressure drop and other constraints. So, considering all the aspects, the objective function for PFHE is formulated as below:

Table 3.8 Process input and physical properties for the PFHE case study

Parameters	Hot side	Cold side
Mass flow rate, m (kg/s)	1.66	2
Inlet temperature, T (°C)	900	200
Density, ρ (kg/m^3)	0.6296	0.9638
Specific heat, C_p (J/kg K)	1122	1073
Viscosity, μ (N s/m^2)	4.01E−05	3.36E−05
Prandtl number, Pr	0.731	0.694

Table 3.9 Lower and upper bounds of design variables for PFHE optimization

Design variables	Lower bound	Upper bound
Cold flow length, L_c (m)	0.1	1
Hot flow length, L_h (m)	0.1	1
Fin height, H (mm)	2	10
Fin thickness, t (mm)	0.1	0.2
Fin frequency, n (m − 1)	100	1000
Fin offset length, l_f (mm)	1	10

Table 3.10 Economic parameters of PFHE

Cost per unit area, C_A (\$/m^2)	90
Electricity price, ζ (\$/MWh)	20
Hours of operation, τ (h)	5000
Nonlinear exponent, n_1	0.6
Depreciation time, z_1 (year)	10
Compressor efficiency, η	0.6
The rate of interest, roi	0.1

$$\begin{cases} \text{Minimize} f(X) = C_{\text{tot}}(X) + \sum_{j=1}^{n} G_1\left(g_j(X)\right)^2 \\ X = [x_1, x_2, x_3, \ldots x_D], \quad x_{\text{i,minimum}} \le x_i, \le x_{\text{i,maximum}}, \quad i = 1, 2, 3, \ldots D \\ g_j(X) \le 0, \quad j = 1, 2, 3, \ldots n \end{cases} \tag{3.75}$$

where X is the vector of design variables which should be bounded between its minimum and maximum values. G_1 is the penalty parameter, and entire term takes into account the effect of constraints violation. This term comes into the picture when the constraint violation takes place. $g_j(X)$ indicates the constraints. The following constraints are considered for the PFHE.

$$0.134 < \alpha < 0.997 \tag{3.76}$$

$$0.012 < \delta < 0.048 \tag{3.77}$$

$$120 < Re < 10^4 \tag{3.78}$$

$$0.041 < \gamma < 0.121 \tag{3.79}$$

$$\Delta P_h \leq 9.5\,\text{kPa} \tag{3.80}$$

$$\Delta P_c \leq 8\,\text{kPa} \tag{3.81}$$

$$T_W \leq 500\,\text{kg} \tag{3.82}$$

The next section describes the results and discussion of the case study.

3.2.3 Results and Discussion

The considered problem of PFHE is investigated using 11 different metaheuristic approaches to obtain a minimum total annual cost. Each algorithm is implemented 100 times on the considered problem to estimate the statistical variations of the algorithms. Each algorithm is implemented with the population size of 50, and the termination criteria are set as 100,000 function evaluations. The results obtained using each algorithm are presented in the form of the best solution, the worst solution, average solution, standard deviation, and success rate obtained in 100 runs in Table 3.11. Here, the solutions which are infeasible (i.e., affected by penalty) are eliminated while obtaining the worst solution, average solution, standard deviation, and success rate. Further, the success rate of the algorithm is obtained by considering 0.1% variation from the global optimum value.

Table 3.11 Comparative results of different algorithms for PFHE optimization

Algorithms	Best	Worst	Average	SD	Success rate (%)
GA	937.9	994.9	964.1	15.0	00
PSO	931.0	994.9	971.6	22.1	00
DE	927.5	929.9	927.7	0.5	93
ABC	927.7	997.8	969.6	21.6	04
CSA	927.5	929.6	927.8	0.5	88
TLBO	927.5	935.5	928.9	2.1	56
SOS	927.5	934.3	929.0	1.7	52
WWO	933.8	1162.1	998.1	53.3	00
HTS	927.5	929.6	927.7	0.6	84
PVS	927.5	928.0	927.7	0.1	92
SCA	928.7	941.0	932.5	2.7	00

It can be observed from the comparative results that DE, PVS, CSA, TLBO, SOS, and HTS performed equally good and produced minimum total annual cost design of PFHE as compared to other algorithms. However, the average performance of DE, PVS, and HTS is better as compared to other competitive algorithms. Further, the success rate of DE algorithm in obtaining the optimum value is the highest followed by the PVS algorithm. The GA, PSO, WWO, and SCA algorithms are unable to obtain the optimum value and hence produced zero success rate. It can be observed from the results that it is difficult to judge the performance of the algorithm as all the algorithms have produced a different performance to obtain the best, worst, and average results, and success rate. So, the Friedman rank test is implemented to judge the best suitable algorithm for PFHE design considering the capability to obtain the best, worst, and average solutions, and success rate. The results of the Friedman rank test are presented in Table 3.12, and its graphical representation is given in Fig. 3.6. The results are presented in the form of Friedman value, normalized value with '1' as the best performing algorithm and its rank. It is observed from the results that DE has obtained the first rank followed by PVS and CSA.

The optimized design of PFHE obtained using the DE is presented in Table 3.13. It can be noted from the results that the higher cold-side flow length is observed as compared to hot-side flow length in optimum PFHE design. However, the pressure drop on both the sides of the heat exchanger is identical because of the mass flow rate and free flow area. Also, the expenditure of capital cost is approximately 73.19%, while remaining expenditure is related to the operating cost in optimized PFHE design. Further, all the constraints are satisfied within the specified limits in the optimized design.

Table 3.12 Friedman rank test results for PFHE optimization

Algorithm	Friedman value	Normalized value	Rank
GA	45	0.23333	9
PSO	47	0.2234	10
DE	10.5	1	1
ABC	42	0.25	8
CSA	12	0.875	3
TLBO	25	0.42	5
SOS	27	0.38889	6
WWO	52.5	0.2	11
HTS	19	0.55263	4
PVS	11.5	0.91304	2
SCA	38.5	0.27273	7

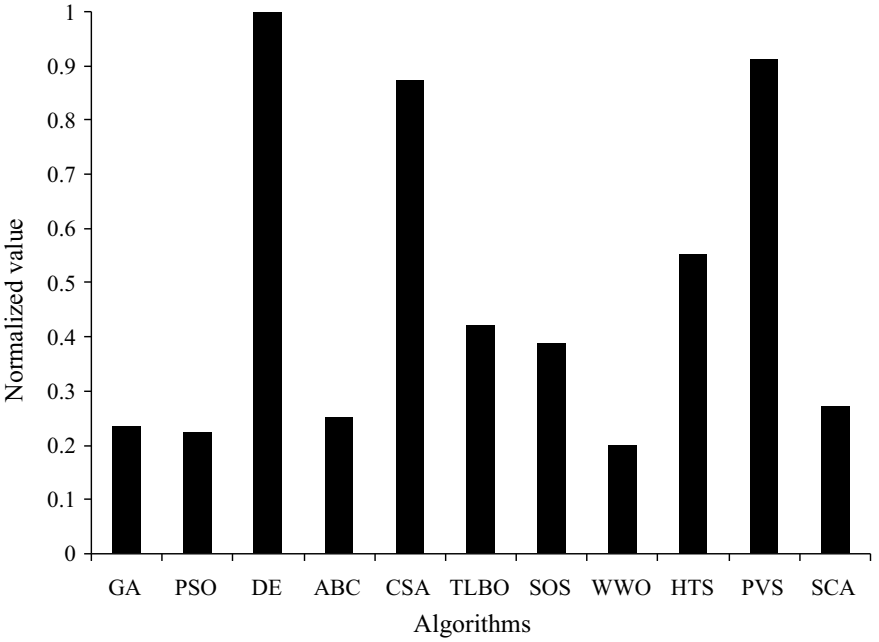

Fig. 3.6 Graphical presentation of Friedman rank test for PFHE optimization

Table 3.13 Optimized plate-fin heat exchanger design geometry

Heat exchanger parameter	Optimized value
Design variables	
Hot-side flow length, L_h (m)	0.8363
Cold-side flow length, L_c (m)	1
Fin height, H (mm)	9.986
Fin thickness, t (mm)	0.1927
Fin frequency, n (m^{-1})	204.3
Fin offset length l_f (mm)	5.189
Number of hot-side layer, (N_h)	71
No flow length, L_n (m)	1.5
Effectiveness (%)	82
Constraints	
Hot-side pressure drop, ΔP_h (kPa)	99.67
Cold-side pressure drop, ΔP_c (kPa)	99.67
Total weight, T_W (kg)	349.39
γ	0.041
α	0.4801
δ	0.0371
Reh	381.87

(continued)

Table 3.13 (continued)

Heat exchanger parameter	Optimized value
Rec	647.41
Objective function	
Capital cost, C_{cp} ($)	678.98
Operating cost, C_{op} ($)	248.61
Total cost, C_{tot} ($)	927.59

3.3 Fin and Tube Heat Exchanger (FTHE)

Fin and tube heat exchangers (FTHE) belong to the compact heat exchangers and generally used for gas to liquid heat transfer. In a gas-to-liquid heat exchange, the heat transfer coefficient on the liquid side is generally higher than that on the gas side. Hence, to balance the thermal conductance on both sides, fins are used on the gas side to increase the surface area. Figure 3.7 shows the schematic diagram of FTHE. A finned tube heat exchanger has tubes with fins attached to the outside surface. However, in some applications fins are mounted on the inside surface of tubes also. Usually, liquid flows through the tubes and air, or some other gas flows outside the tubes. Fins are radial for cross-flow fin and tube arrangement. For counter-flow or parallel flow FTHE, the fins should be longitudinal instead of radial. Depending on the type of fin, FTHEs are: FTHE having normal fins on individual tubes, FTHE having flat fins, the fins can be plain, wavy, or interrupted, and the tubes can be circular, oval, or rectangular shapes, and longitudinal fins on individual tubes.

The major advantages of FTHE are wide application and temperature spectrum, handle low heat transfer coefficient fluids, and high tube-side velocity prevents fouling inside the tubes. At the same time, some drawbacks are also associated with FTHE like it cannot handle slurry fluids, deposition of the particle at fin corner reduces the heat transfer rate, cleaning is difficult, and high-pressure drop. Finned tube heat exchangers are often used in power plants as a preheating and exhaust gas heat exchanger. In industrial dryers, finned tube heat exchangers are used for heating of air. Apart from these, FTHEs are also used in power and chemical engineering applications such as compressors, intercoolers, air coolers, and fan coils because of their high compactness and relatively good heat transfer efficiency.

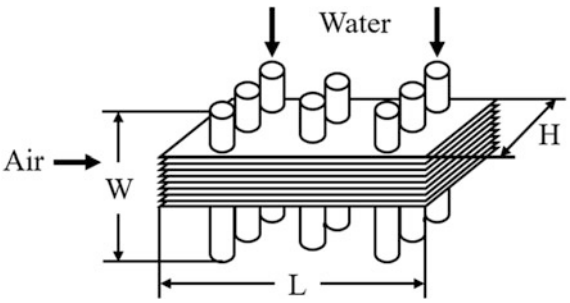

Fig. 3.7 Schematic diagram of fin and tube heat exchanger